GOVERNMENT DEGREE COLLEGE, CHODAVARAM

ANAKAPALLI DISTRICT

PAPER PUBLICATIONS

1.

Journal of Inorganic and Organometallic Polymers and Materials
https://doi.org/10.1007/s10904-020-01773-6

Evaluation of Structural, Micro-structural, Vibrational and Elastic Properties of Ni–Cu–Zn Nanoferrites: Role of Dopant Cu^{2+} at Constant 0.1 mol% in Ni–Zn Spinel Structure

K. S. Ramakrishna[1] · Ch. Srinivas[2] · S. A. V. Prasad[2] · E. Ranjith Kumar[3] · K. Ramachandra Rao[4] · C. L. Prajapat[5,6] · T. V. Chandrasekhara Rao[5] · Sher Singh Meena[7] · D. L. Sastry[8]

Received: 9 August 2020 / Accepted: 26 September 2020

Abstract
Structural and elastic properties have been investigated for a series of heat treated $Ni_xCu_{0.1}Zn_{0.9-x}Fe_2O_4$ ($x = 0.5, 0.6, 0.7$) nanoferrite powders which were synthesized using co-precipitation method. Rietveld refinement patterns revealed the spinel phase belonging to *fd3m* space group. Lattice parameters of the heat treated samples are in the range of (8.453–8.417 Å). As the substitution level of Ni^{2+} increased, the lattice parameter decreased in the samples sintered at 200 °C, but it was randomly varied in the in the samples sintered at 500 °C. The average crystallite size (4.1–10.9 nm) estimated from XRD as well as average particle size (5.5–11.3 nm) estimated from FE-SEM were found to be increased with the increase of Ni^{2+} ion concentration in sintered ferrite samples. Sintering process was promoting the growth of nanoparticle size. The spherical nature of ferrite nanoparticles was evident from the FE-SEM micrographs. The vibrational bands observed in the FTIR spectra confirm the cubic spinel phase of ferrite systems. The variation of vibrational bands seems to be dependent on the particular metal ion occupying the spinel structure rather than the changes in bond lengths of Fe^{3+}–O^{2-} ion complexes. The present values of elastic moduli revealed the mechanical hardness of present heat treated ferrite samples. Interestingly, the elastic moduli depend upon the variation of both inter-atomic distances as well as cation redistribution. The identical value of Poisson's ratio (0.35) is an authentication of isotropic behaviour of the present ferrite systems.

Keywords Ferrite nanoparticles · Cation redistribution · Vibrational frequencies · Elastic moduli · Lattice energy

2

Journal of Alloys and Compounds
Volume 852, 25 January 2021, 156967

Influence of Ge^{4+} doping on photo- and electroluminescence properties of $ZnGa_2O_4$

Ch. Satya Kamal [a], R.K. Mishra [c], K. Ramachandra Rao [b], Bal Govind Vats [d], M.V. Pimple [c], V. Sudarsan [c], R.K. Vatsa [c]

https://doi.org/10.1016/j.jallcom.2020.156967

Abstract

Nanocrystalline $ZnGa_2O_4$ samples doped with varying concentrations of Ge^{4+} ions were prepared and their photo- and electroluminescence properties were investigated in detail before and after annealing at 900°C. X-ray diffraction (XRD) studies confirmed that Ge^{4+} doping even to a level of 0.5 at.% at the expense of Ga^{3+} in $ZnGa_2O_4$ leads to incorporation of significant extent Ga^{3+} ions (~29%) at Zn^{2+} site (tetrahedral site) in $ZnGa_2O_4$ lattice thereby increasing relative extent of distorted gallium-oxygen (GaO_x) structural units. XRD, UV-Visible optical reflectance and lifetime measurements confirmed that a maximum of 0.65 at.% Ge^{4+} is doped in nanocrystalline $ZnGa_2O_4$. Observed blue shift in photoluminescence maximum and decrease in line width with Ge^{4+} doping is explained based on increased electro-negativity of Ge^{4+} compared to Ga^{3+} and lack of formation of oxygen vacancies particularly for 900°C annealed samples. Lack of oxygen vacancies in Ge^{4+} doped annealed samples facilitates selective excitation of regular GaO_6 and GaO_x structural units, upon application of AC voltages, leading to around 50% reduction in line width of electroluminescence peak from doped sample compared to undoped one. Observed variation in electroluminescence properties between doped and undoped samples have been understood based on difference in nature of defects generated in the lattice.

3.

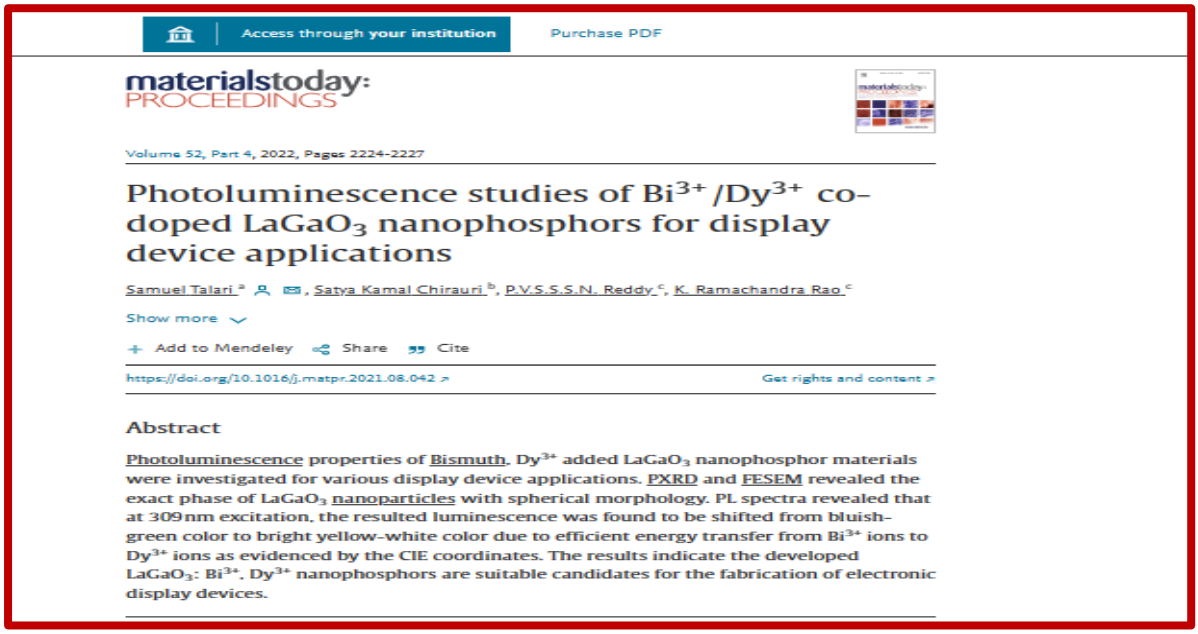

Access through your institution | Purchase PDF

materialstoday: PROCEEDINGS

Volume 52, Part 4, 2022, Pages 2224-2227

Photoluminescence studies of Bi^{3+} /Dy^{3+} co-doped $LaGaO_3$ nanophosphors for display device applications

Samuel Talari [a], Satya Kamal Chirauri [b], P.V.S.S.S.N. Reddy [c], K. Ramachandra Rao [c]

Show more

Add to Mendeley | Share | Cite

https://doi.org/10.1016/j.matpr.2021.08.042 | Get rights and content

Abstract

Photoluminescence properties of Bismuth. Dy^{3+} added $LaGaO_3$ nanophosphor materials were investigated for various display device applications. PXRD and FESEM revealed the exact phase of $LaGaO_3$ nanoparticles with spherical morphology. PL spectra revealed that at 309 nm excitation, the resulted luminescence was found to be shifted from bluish-green color to bright yellow-white color due to efficient energy transfer from Bi^{3+} ions to Dy^{3+} ions as evidenced by the CIE coordinates. The results indicate the developed $LaGaO_3$: Bi^{3+}, Dy^{3+} nanophosphors are suitable candidates for the fabrication of electronic display devices.

4.

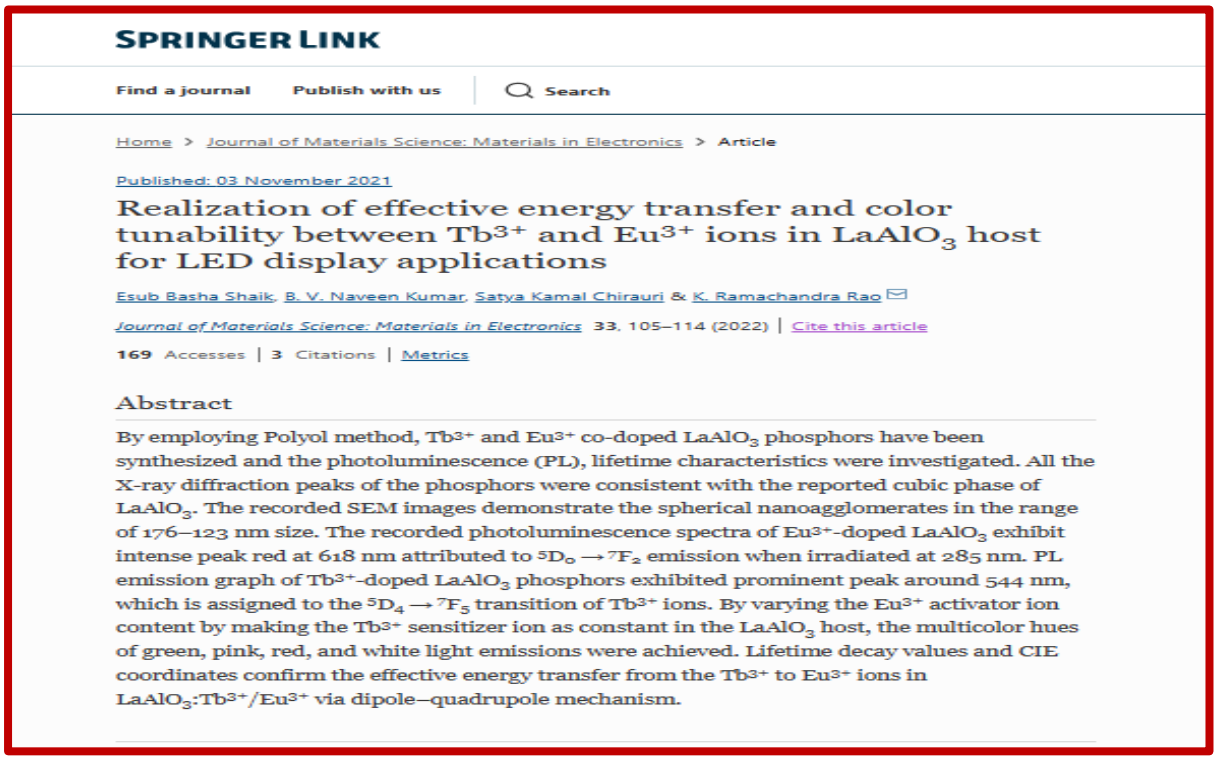

SPRINGER LINK

Find a journal | Publish with us | Search

Home > Journal of Materials Science: Materials in Electronics > Article

Published: 03 November 2021

Realization of effective energy transfer and color tunability between Tb^{3+} and Eu^{3+} ions in $LaAlO_3$ host for LED display applications

Esub Basha Shaik, B. V. Naveen Kumar, Satya Kamal Chirauri & K. Ramachandra Rao

Journal of Materials Science: Materials in Electronics 33, 105–114 (2022) | Cite this article

169 Accesses | 3 Citations | Metrics

Abstract

By employing Polyol method, Tb^{3+} and Eu^{3+} co-doped $LaAlO_3$ phosphors have been synthesized and the photoluminescence (PL), lifetime characteristics were investigated. All the X-ray diffraction peaks of the phosphors were consistent with the reported cubic phase of $LaAlO_3$. The recorded SEM images demonstrate the spherical nanoagglomerates in the range of 176–123 nm size. The recorded photoluminescence spectra of Eu^{3+}-doped $LaAlO_3$ exhibit intense peak red at 618 nm attributed to $^5D_0 \rightarrow {}^7F_2$ emission when irradiated at 285 nm. PL emission graph of Tb^{3+}-doped $LaAlO_3$ phosphors exhibited prominent peak around 544 nm, which is assigned to the $^5D_4 \rightarrow {}^7F_5$ transition of Tb^{3+} ions. By varying the Eu^{3+} activator ion content by making the Tb^{3+} sensitizer ion as constant in the $LaAlO_3$ host, the multicolor hues of green, pink, red, and white light emissions were achieved. Lifetime decay values and CIE coordinates confirm the effective energy transfer from the Tb^{3+} to Eu^{3+} ions in $LaAlO_3$:Tb^{3+}/Eu^{3+} via dipole–quadrupole mechanism.

5.

Chimica Techno Acta
published by Ural Federal University
eISSN 2411-1414; chimicatechnoacta.ru

ARTICLE
2022, vol. 9(1), No. 20229107
DOI: 10.15826/chimtech.2022.9.1.07

Bright blue emissions on UV-excitation of $LaBO_3$ (B=In, Ga, Al) perovskite structured phosphors for commercial solid-state lighting applications

B.V. Naveen Kumar [ab], T. Samuel [c], Samatha Bevara [d], K. Ramachandra Rao [e], Satya Kamal Chirauri [e*]

a: Department of Physics, Acharya Nagarjuna University, Guntur, India
b: Shri Vishnu College of Engineering for Women(A), Bhimavaram, India
c: GMR Institute of Technology, Rajam, Andhra Pradesh, India
d: Chemistry Division, Vignan's Foundation for Science, Technology and Research, Guntur, Andhra Pradesh, India
e: Crystal Growth & Nanoscience Research Center, Government College (A), Rajahmundry, India
* Corresponding author: satyakamal.ch@gmail.com

This article belongs to the regular issue.

Abstract

Bright blue photoluminescence (PL) was obtained from Bi^{3+}-activated $LaBO_3$ (B = In, Ga, Al) perovskite nanophosphors. A cost-effective and low-temperature chemical route was employed for preparing Bi^{3+} doped $LaBO_3$ (B=In, Ga, Al) which were then annealed at 1000 °C. The phase formation, morphological studies and luminescent properties of the as-prepared samples were performed by X-ray diffraction (XRD), scanning electron microscopy (SEM), photoluminescence and optical absorption spectroscopy. Comparison of emission intensities, lifetime studies, energy band gaps and color purity of all samples (pure and Bi^{3+} doped) were investigated for promising applications in UV light-emitting diodes, variable frequency drive (VFD), field emission display (FED), and other photoelectric fields.

Keywords
perovskites
photoluminescence
phosphor
quenching
solid-state lightning

Received: 08.07.2021
Revised: 02.01.2022
Accepted: 04.03.2022
Available online: 11.03.2022

6.

LUMINESCENCE

RESEARCH ARTICLE

Tunable luminescence from Bi^{3+} sensitized $La_2Zr_2O_7:Eu^{3+}$ red nanophosphors for display applications

Basina Veera Naveen Kumar, Kankanala Venkata Rao, Esub Basha Shaik, Yerramala Nirmal Rajeev, Kokkirapati Ramachandra Rao, Sandhya Cole

First published: 05 September 2022 | https://doi.org/10.1002/bio.4378 | Citations: 1

Read the full text > PDF TOOLS SHARE

Abstract

Bismuth ion (Bi^{3+}) sensitized, europium ion (Eu^{3+}) activated $La_2Zr_2O_7$ nanophosphors are prepared successfully by simple wet chemical method. Strong blue emission of singly doped $La_2Zr_2O_7$ with Bi^{3+} was observed at 310 nm excitation, its wide emission spectrum has a peak maximum at 465 nm ascribed to electronic transition $^3P_1 \rightarrow {}^1S_0$ of Bi^{3+}. The recorded photoluminescence spectra of y at% Eu^{3+} codoped $La_2Zr_2O_7$, when excited at 285 nm, the emission spectrum exhibits maximum peaks at wavelength values 615 nm, 646 nm and 665 nm which are ascribed to $^5D_0 \rightarrow {}^7F_2$, $^5D_0 \rightarrow {}^7F_3$ and $^5D_0 \rightarrow {}^7F_4$ transitions of Eu^{3+} respectively. The chromaticity coordinates for the optimized sample were found to be (0.519, 0.329). Sensitizing with Bi^{3+} can affect the luminescence properties of $La_2Zr_2O_7:Eu^{3+}$ phosphors. With reference to the change in Eu^{3+} concentration from Y = 1, 2, 3, 4 and 5%, color tunable luminescence from blue to orange, red of $La_2Zr_2O_7:Bi^{3+},Eu^{3+}$ phosphors are observed. The lifetime decay values, energy level description and CIE chromatic color coordinates for Bi^{3+}, Eu^{3+} in $La_2Zr_2O_7:Bi^{3+},Eu^{3+}$ codoped sample was discussed. The spectral overlap between sensitizer, activator ions confirms the efficient energy transfer from Bi^{3+} to Eu^{3+} in $La_2Zr_2O_7:Bi^{3+},Eu^{3+}$ codoped sample and is via a dipole-quadruple mechanism.

7.

SPRINGER LINK

Find a journal | Publish with us | Search

Home > Acta Geophysica > Article

Research Article - Atmospheric & Space Sciences | Published: 03 March 2022

Increasing pre-monsoon rain days over four stations of Kerala, India

Nandivada Umakanth, S. S. S. Kalyan, Gubbala China Satyanarayana, Rajesh Gogineni, Ayachithula Nagarjuna, Ramisetti Naveen, Kokkerapati Ramachandra Rao & Myla Chimpiri Rao

Acta Geophysica **70**, 963–978 (2022) | Cite this article

233 Accesses | Metrics

Abstract

The climate of India varies greatly by region, as seen by wind patterns, temperature and rainfall, seasonal rhythms and the degree of wetness or dryness. During the several seasons, the weather conditions change. Changes in meteorological factors (temperature, pressure, wind direction and velocity, humidity and precipitation, etc.) cause these changes. The pre-monsoon season (PRMS) comprises of March, April and May months. The precipitation patterns observed in PRMS are crucial because it affects a variety of crop-related operations across the country. The lifting index (LI), K index (KI), total totals index (TTI), humidity index (HI), improved k index, improved total totals index, total precipitable water (TPW) and convective available potential energy (CAPE) are studied at four locations in Kerala during PRMS. These variables were examined on rain day (RD)'s and no rain day (NRD)'s. The four stations we chose for our investigation were Thiruvananthapuram, Kochi, Alappuzha and Kannur. The GPM IMERG (Integrated Multi-satellite Retrievals for Global Precipitation Measurement) daily rainfall datasets have been utilized for this analysis. Fifth-generation ECMWF atmospheric reanalysis (ERA5) daily data for the PRMS of 2021 were used to measure all rainfall-related variables. During PRMS, all metrics clearly distinguished the RD and NRD. The rise in relative humidity and observations of dew point depression indicates that there is enough moisture for convective rain. In May, there were more negative VV values than in April.

8.

Physical Chemistry Research

Home | Browse | Journal Info | Guide for Authors | Submit Manuscript | Reviewers | Contact Us

Structural and Morphological Studies on Strontium Tin Phosphate SrSn(PO4)2 Nanopowder

Document Type : Regular Article

Authors

Y Nirmal Rajeev [1]; Venkatarao K [2]; B.V. Naveen Kumar [3]; L. Bhushan Kumar [4]; Sandhya Cole [4]

[1] Dept of Physics, Acharya Nagarjuna University, Guntur 522 510, India. Dept of Physics, V.R. Siddhartha Engineering College, Vijayawada 520 007, India

[2] Dept of Physics, Acharya Nagarjuna University, Guntur 522 510, India. Dept of Physics, Government Polytechnic College, Krosuru 522 410, India

[3] Dept of Physics, Acharya Nagarjuna University, Guntur 522 510, India. Dept of Physics, BVC College of Engineering, Rajahmundry 5333 102, India

[4] Dept of Physics, Acharya Nagarjuna University, Guntur 522 510, India

10.22036/PCR.2021.300514.1953

Abstract

Strontium Tin phosphate SrSn(PO4)2 nanopowder was prepared by simple Solid State Reaction method (SSR). Structural and morphological investigations of the synthesized nanopowder were characterized by Powdered X-ray diffraction study (P-XRD), Fourier transform infrared (FT-IR) Spectroscopy, Field Emission Scanning Electron Microscopy (FE-SEM) and Energy Dispersive X-ray Spectroscopy Analysis (EDS). The average crystallite size estimated from P-XRD study was around 17 nm. W-H plot method was also agreed the size of the crystallite of the prepared sample in nanoscale. FE-SEM images show agglomerates of non-uniform biscuit like nano flakes structure. Various functional groups of prepared sample exhibited phosphate related bands are confirmed by FT-IR study.

9.

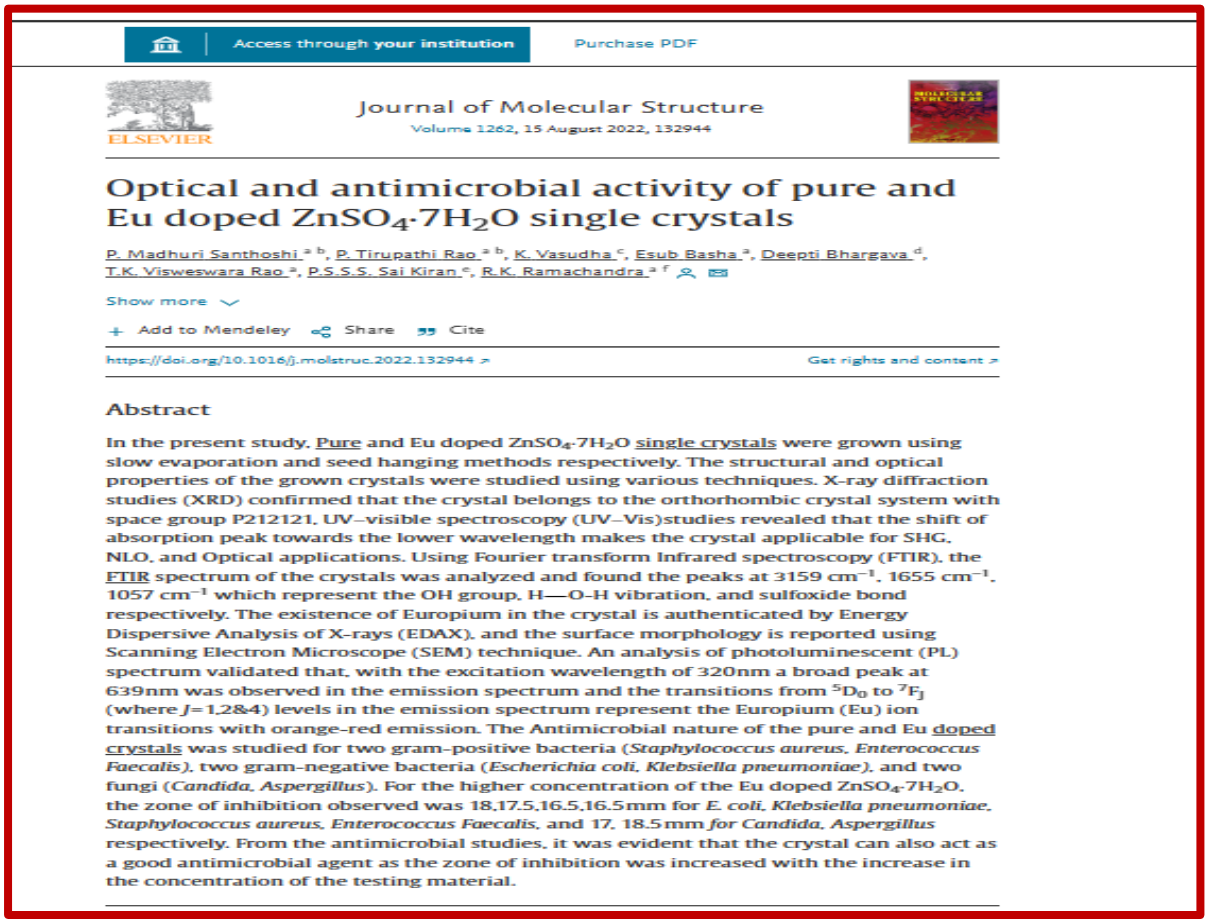

Access through your institution Purchase PDF

Journal of Molecular Structure
Volume 1262, 15 August 2022, 132944

Optical and antimicrobial activity of pure and Eu doped $ZnSO_4 \cdot 7H_2O$ single crystals

P. Madhuri Santhoshi [a b], P. Tirupathi Rao [a b], K. Vasudha [c], Esub Basha [a], Deepti Bhargava [d], T.K. Visweswara Rao [a], P.S.S.S. Sai Kiran [e], R.K. Ramachandra [a f]

Show more

Add to Mendeley Share Cite

https://doi.org/10.1016/j.molstruc.2022.132944 Get rights and content

Abstract

In the present study, Pure and Eu doped $ZnSO_4 \cdot 7H_2O$ single crystals were grown using slow evaporation and seed hanging methods respectively. The structural and optical properties of the grown crystals were studied using various techniques. X-ray diffraction studies (XRD) confirmed that the crystal belongs to the orthorhombic crystal system with space group P212121. UV–visible spectroscopy (UV–Vis)studies revealed that the shift of absorption peak towards the lower wavelength makes the crystal applicable for SHG, NLO, and Optical applications. Using Fourier transform Infrared spectroscopy (FTIR), the FTIR spectrum of the crystals was analyzed and found the peaks at 3159 cm^{-1}, 1655 cm^{-1}, 1057 cm^{-1} which represent the OH group, H—O-H vibration, and sulfoxide bond respectively. The existence of Europium in the crystal is authenticated by Energy Dispersive Analysis of X-rays (EDAX), and the surface morphology is reported using Scanning Electron Microscope (SEM) technique. An analysis of photoluminescent (PL) spectrum validated that, with the excitation wavelength of 320nm a broad peak at 639nm was observed in the emission spectrum and the transitions from $^5D_0$ to ^7F_J (where J=1,2&4) levels in the emission spectrum represent the Europium (Eu) ion transitions with orange–red emission. The Antimicrobial nature of the pure and Eu doped crystals was studied for two gram-positive bacteria (*Staphylococcus aureus, Enterococcus Faecalis*), two gram-negative bacteria (*Escherichia coli, Klebsiella pneumoniae*), and two fungi (*Candida, Aspergillus*). For the higher concentration of the Eu doped $ZnSO_4 \cdot 7H_2O$, the zone of inhibition observed was 18,17.5,16.5,16.5mm for *E. coli, Klebsiella pneumoniae, Staphylococcus aureus, Enterococcus Faecalis*, and 17, 18.5mm *for Candida, Aspergillus* respectively. From the antimicrobial studies, it was evident that the crystal can also act as a good antimicrobial agent as the zone of inhibition was increased with the increase in the concentration of the testing material.

10.

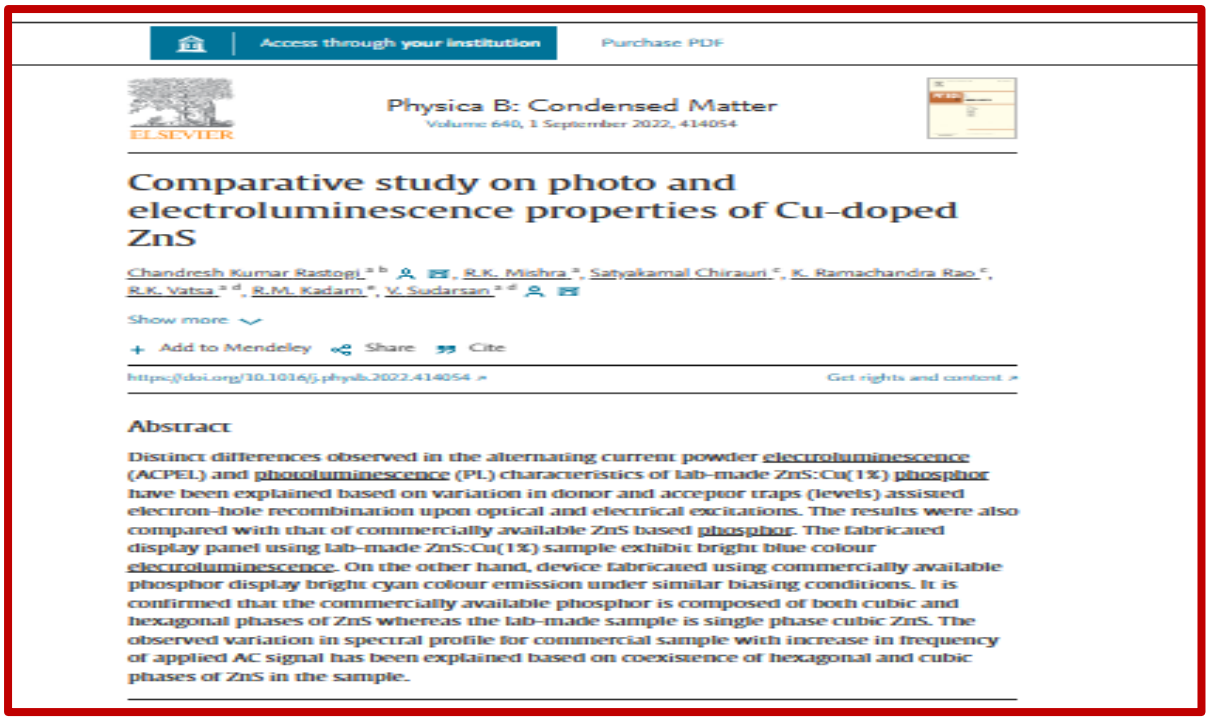

Access through your institution Purchase PDF

Physica B: Condensed Matter
Volume 640, 1 September 2022, 414054

Comparative study on photo and electroluminescence properties of Cu-doped ZnS

Chandresh Kumar Rastogi [a b], R.K. Mishra [a], Satyakamal Chirauri [c], K. Ramachandra Rao [c], R.K. Vatsa [a d], R.M. Kadam [e], V. Sudarsan [a d]

Show more

Add to Mendeley Share Cite

https://doi.org/10.1016/j.physb.2022.414054 Get rights and content

Abstract

Distinct differences observed in the alternating current powder electroluminescence (ACPEL) and photoluminescence (PL) characteristics of lab-made ZnS:Cu(1%) phosphor have been explained based on variation in donor and acceptor traps (levels) assisted electron–hole recombination upon optical and electrical excitations. The results were also compared with that of commercially available ZnS based phosphor. The fabricated display panel using lab-made ZnS:Cu(1%) sample exhibit bright blue colour electroluminescence. On the other hand, device fabricated using commercially available phosphor display bright cyan colour emission under similar biasing conditions. It is confirmed that the commercially available phosphor is composed of both cubic and hexagonal phases of ZnS whereas the lab-made sample is single phase cubic ZnS. The observed variation in spectral profile for commercial sample with increase in frequency of applied AC signal has been explained based on coexistence of hexagonal and cubic phases of ZnS in the sample.

11.

Access through your institution | Purchase PDF | Patient Access

Journal of Controlled Release
Volume 352, December 2022, Pages 652-672

Review article

Engineered upconversion nanocarriers for synergistic breast cancer imaging and therapy: Current state of art

Pavan Kumar Chintamaneni [a], Dasari Nagasen [b c], Katta Chanti Babu [d], Atul Mourya [d], Jitender Madan [d], Dadi A. Srinivasarao [d], R.K. Ramachandra [e f], P. Madhuri Santhoshi [e], Sai Kiran S.S. Pindiprolu [b c]

Show more

+ Add to Mendeley | Share | Cite

https://doi.org/10.1016/j.jconrel.2022.10.056 | Get rights and content

Abstract

Breast cancer is the most common type of cancer in women and is the second leading cause of cancer-related deaths worldwide. Early diagnosis and effective therapeutic interventions are critical determinants that can improve survival and quality of life in breast cancer patients. Nanotheranostics are emerging interventions that offer the dual benefit of in vivo diagnosis and therapeutics through a single nano-sized carrier. Rare earth metal-doped upconversion nanoparticles (UCNPs) with their ability to convert near-infrared light to visible light or UV light in vivo settings have gained special attraction due to their unique luminescence and tumor-targeting properties. In this review, we have discussed applications of UCNPs in drug and gene delivery, photothermal therapy (PTT), photodynamic therapy (PDT) and tumor targeting in breast cancer. Further, present challenges and future opportunities for UCNPs in breast cancer treatment have also been mentioned.

12.

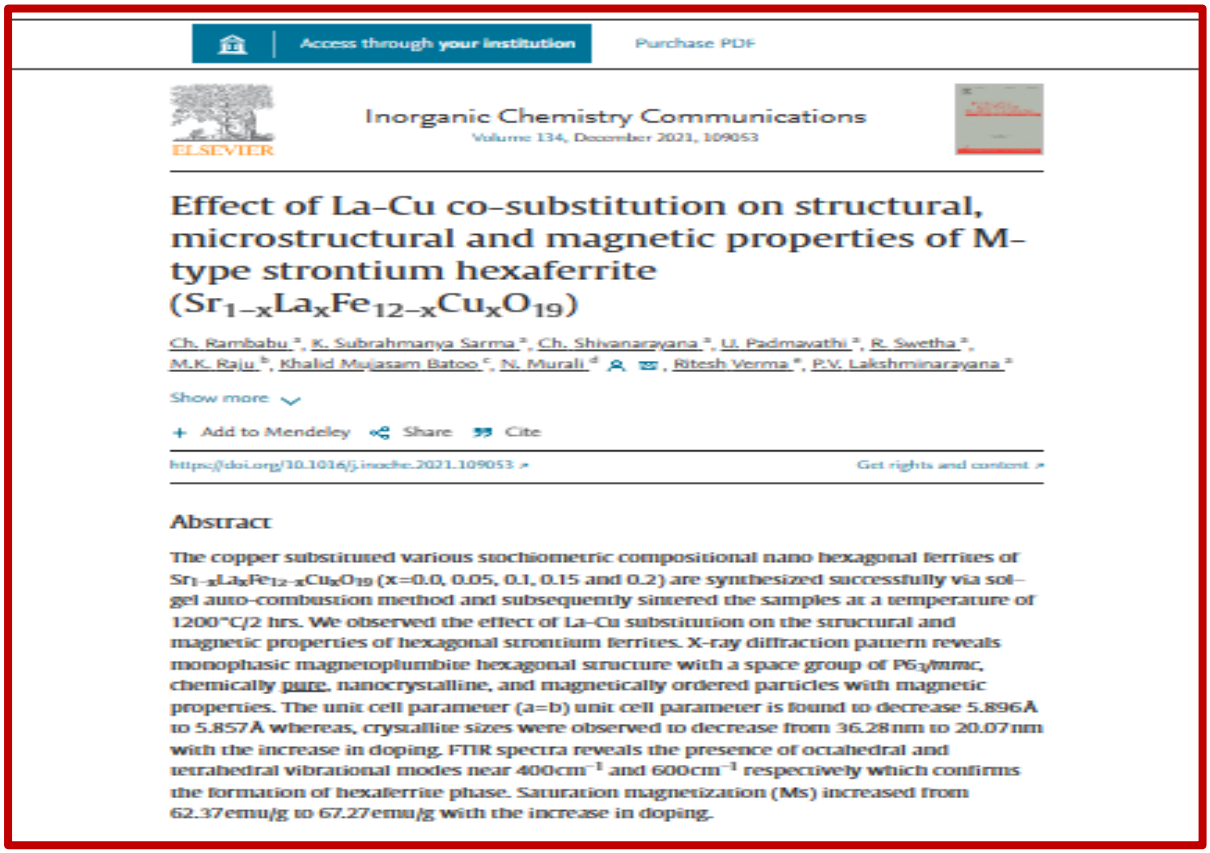

Access through your institution | Purchase PDF

Inorganic Chemistry Communications
Volume 134, December 2021, 109053

Effect of La–Cu co-substitution on structural, microstructural and magnetic properties of M-type strontium hexaferrite ($Sr_{1-x}La_xFe_{12-x}Cu_xO_{19}$)

Ch. Rambabu [a], K. Subrahmanya Sarma [a], Ch. Shivanarayana [a], U. Padmavathi [a], R. Swetha [a], M.K. Raju [b], Khalid Mujasam Batoo [c], N. Murali [d], Ritesh Verma [e], P.V. Lakshminarayana [a]

Show more

+ Add to Mendeley | Share | Cite

https://doi.org/10.1016/j.inoche.2021.109053 | Get rights and content

Abstract

The copper substituted various stochiometric compositional nano hexagonal ferrites of $Sr_{1-x}La_xFe_{12-x}Cu_xO_{19}$ (x=0.0, 0.05, 0.1, 0.15 and 0.2) are synthesized successfully via sol–gel auto-combustion method and subsequently sintered the samples at a temperature of 1200°C/2 hrs. We observed the effect of La–Cu substitution on the structural and magnetic properties of hexagonal strontium ferrites. X-ray diffraction pattern reveals monophasic magnetoplumbite hexagonal structure with a space group of $P6_3/mmc$, chemically pure, nanocrystalline, and magnetically ordered particles with magnetic properties. The unit cell parameter (a=b) unit cell parameter is found to decrease 5.896Å to 5.857Å whereas, crystallite sizes were observed to decrease from 36.28nm to 20.07nm with the increase in doping. FTIR spectra reveals the presence of octahedral and tetrahedral vibrational modes near 400cm^{-1} and 600cm^{-1} respectively which confirms the formation of hexaferrite phase. Saturation magnetization (Ms) increased from 62.37emu/g to 67.27emu/g with the increase in doping.

13.

SPRINGER LINK

Find a journal Publish with us Search

Home > Applied Physics A > Article

Published: 09 December 2021

Enhanced structural and magnetic properties of Al–Cr-substituted $SrFe_{12}O_{19}$ hexaferrite system

K. Subrahmanya Sarma, Ch. Rambabu, G. Vishnu Priya, M. K. Raju, D. Parajuli, Batoo Khalid Mujasam, Verma Ritesh, Kumar Rajesh, N. Murali ✉ & P. V. Lakshminarayana

Applied Physics A **128**, Article number: 26 (2022) | Cite this article

389 Accesses | **6** Citations | Metrics

Abstract

M-type Al–Cr-substituted strontium hexaferrite ($SrFe_{12-x-y}Al_xCr_yO_{19}$ where x = y = 0.0, 0.05, 0.1, 0.15, and 0.2) powders are synthesized successfully using sol–gel auto-combustion method. The synthesized powders were sintered at 1200 °C for 2 h, and their structural, morphological, and magnetic properties were studied using characterization techniques like XRD (X-ray diffraction), FTIR (Fourier transform infrared spectroscopy), SEM (scanning electron microscopy), and VSM (vibrating sample magnetometer). The XRD pattern confirmed the formation of single phase hexagonal structure with $P6_3/mmc$ space group. The saturation magnetization is observed to decrease from 63.37 to 46.89 emu/g with the increase in dopant concentration. However, the coercivity initially decreased and then increased with increase in dopant concentration.

14.

TÜBİTAK

Turkish Journal of Chemistry

http://journals.tubitak.gov.tr/chem/

Research Article

Turk J Chem
(2022) 46: 1972-1983

doi:10.55730/1300-0527.3495

Adsorptive removal of crystal violet from aqueous solution by ultrasonic-assisted synthesized zirconium-2,6-naphthalenedicarboxylate metal-organic framework

Penmethsa Kiran KUMAR[1,2], **Sunkara Satya VENI**[2,*]

[1]Department of Chemistry, Government Degree College, Chodavaram, Andhra Pradesh, India
[2]Department of Chemistry, Jawaharlal Nehru Technological University Kakinada, Kakinada, Andhra Pradesh, India

Received: 28.05.2022 • **Accepted/Published Online:** 23.08.2022 • **Final Version:** 19.12.2022

Abstract: Zirconium-2,6-naphthalenedicarboxylate metal-organic framework (Zr-NDC MOF) was prepared using ultrasound-assisted synthesis and tested for the adsorptive removal of crystal violet (CV) dye from aqueous solution. The pristine Zr-NDC was characterized using powder X-ray diffraction, scanning electron microscopy, thermogravimetric analysis, and energy-dispersive X-ray spectroscopy, Fourier-transform infrared, elemental analysis, and dynamic light scattering techniques. The maximum percentage removal of CV dye was found to be 99.45% with an initial dye concentration of 10 mg L^{-1}. The kinetics and adsorption isotherm models were used to investigate the removal of CV dye from aqueous solution using Zr-NDC. Langmuir adsorption isotherm model ($R^2 = 0.9880$) describes the adsorption of CV dye onto Zr-NDC and the maximum equilibrium adsorption capacity (454.2 mg g^{-1}) was achieved with the CV dye having an initial concentration of 100 mg L^{-1}. The adsorption was found to follow pseudo-second-order kinetics ($R^2 = 0.9960$) with a rate constant of 6.52×10^{-4} g mg^{-1} min^{-1}. The effect of various parameters such as dye concentration, contact time, pH of dye solution, and MOF dose on the adsorption of dye was investigated. The study proved that the Zr-NDC is a promising adsorbent in the removal of CV dye from aqueous solution.

Key words: Adsorption, crystal violet, metal-organic framework, ultrasound-assisted, zirconium